

**Proceedings of the
Sixth International Conference on
Engineering Computational Technology**

**Edited by
M. Papadrakakis and B.H.V. Topping**



**Athens - Greece
2-5 September 2008**

CIVIL-COMP PRESS

© Civil-Comp Ltd, Stirlingshire, Scotland

published 2008 by

Civil-Comp Press

Dun Eaglais, Kippen

Stirlingshire, FK8 3DY, UK

Civil-Comp Press is an imprint of Civil-Comp Ltd

ISBN 978-1-905088-24-9 (Book)

ISBN 978-1-905088-25-6 (CD-Rom)

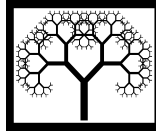
ISBN 978-1-905088-26-3 (Combined Set)

British Library Cataloguing in Publication Data

A catalogue record for this book is available from the British Library

Cover Image: mesh created by R. Montenegro and G. Montero based on the "25 Years of Civil-Comp Conferences" logo.

Printed in Great Britain by Bell & Bain Ltd, Glasgow



Phase Transformations in Finite Length Nanowires: Analysis with Mesoscopic Models

L.X. Wang¹ and R. Melnik²

¹ Faculty of Mechanical Engineering

Hangzhou Dainzi University, Xiasha, Hangzhou, P.R. China

² M²NeT Lab

Wilfrid Laurier University, Waterloo, Canada

Abstract

It is known that in gold (Au) nanowires, the energy as a function of lattice spacing exhibits two distinct minima that correspond to fcc and bct phases. These, as well as other nanowires based on ZnO, Cu, Ni, Al, Ag, can exhibit what is known as shape memory effects. However, most theoretical and computational results up to date concern infinitely long nanowires. From a computational point of view, studies of finite length nanowires are more demanding and the development of efficient methodologies is required for success. In this contribution, our focus is on nanowires of finite length. We provide details on several computational experiments aimed at the analysis of square-to-rectangle phase transformations in such nanostructures. We base our considerations on a modification of the coupled system of partial differential equations for the evolution of displacements and temperature in the structure.

Keywords: phase transformations, nanowires, FVM, POD, biomolecule and entropic elasticity, nonlocal models and nanostructures.

1 Introduction

Recently, experiments on gold (Au) nanowires demonstrated that they can exhibit shape memory effects. This has been confirmed computationally with several different methodologies, including tight-binding and density functional theory [1]. Shape memory effects have also been observed in ZnO nanowires as well as in other types of nanowires that show substantial potential for many applications in nano- and biotechnology, including Cu, Ni, Al, Ag (see, e.g., [2]).

While many results up to date have been obtained for infinitely long nanowires (as well as for infinitely large nanoplates), including those obtained with ab initio cal-

culations, the question has remained on whether phase transformations is a generic phenomenon for the same material-type nanowires of finite length. This question is of utmost practical importance due to an increasing range of current and potential applications of nanowire structures. Recently, there has been mounting evidence towards a positive answer to this question [10]. However, comprehensive studies of nanowires of finite length are limited due to the fact that the methodologies applied for their studies are computationally expensive. In addition, there are a number of questions that remain open at a large extent, including questions related to temperature-dependent phase stability.

In a series of recent papers we developed several efficient methodologies to solve 2D models describing square-to-rectangle phase transformations in materials with memory, in particular the finite volume methodology [9] and a numerical reduction procedure based on the Proper Orthogonal Decomposition (POD) [8]. However, since the original model here has been simplified, in this contribution we discuss the application of a modified procedure which is being applied to the analysis of gold (Au), iron-based (FePd), and zinc-based oxide (ZnO) nanowires. The results presented here are for Cu nanowires that have the same length but different diameters. Typical results for different diameter-length ratios are discussed and observed phenomena are explained.

2 Free Energy of Square to Rectangular Transformations

Since our main focus on nanowires, we limit ourselves to the two-dimensional case where square to rectangle transformations provide a generic counterpart of cubic to tetragonal as well as tetragonal to orthorhombic transformations. In this case, the free energy of the system can be represented as follows (e.g. [8]):

$$\Psi = \frac{a_1}{2}e_1^2 + \frac{a_3}{2}e_3^2 + \frac{A_2}{2}e_2^2 + \frac{a_4}{4}e_2^4 + \frac{a_6}{6}e_2^6 + \frac{k}{2}(\|\nabla e_2\|)^2, \quad (1)$$

where $A_2, a_i \quad i = 1, \dots, 6, d_2$, and d_3 are the material-specific coefficients, and e_1, e_2, e_3 are dilatational, deviatoric, and shear components of the strains, respectively, which are defined as follows:

$$e_1 = (\eta_{11} + \eta_{22}) / \sqrt{2}, \quad (2)$$

$$e_2 = (\eta_{11} - \eta_{22}) / \sqrt{2}, \quad (3)$$

$$e_3 = (\eta_{12} + \eta_{21}) / 2. \quad (4)$$

The Cauchy-Lagrangian strain tensor $\boldsymbol{\eta}$ is given by its components in the standard manner with the repeated-index convention used:

$$\eta_{ij} = (u_{i,j} + u_{j,i}) / 2 \quad (5)$$

where u_i is the displacement in the i^{th} direction in the coordinate system, $u_{i,x}$ stands for $\partial u_i / \partial x$ and similarly for all other variables. \mathbf{x} is the coordinates of a material point in the domain of interest. In this free energy function, the deviatoric strain e_2 is chosen as the order parameter.

3 Governing Equations

In this contribution, we develop a relatively simple and computationally inexpensive model to study phase transformations in finite nanostructures with our major focus given here to nanowires of finite length. In the latter case, the models describing shape memory effects at the mesoscopic level such as those developed in [5, 3, 4] can be reduced to a 2D case (and in the case of nanowires of infinite length, to the 1D case). Since our interest also lies with the cubic-to-tetragonal transformations, we consider its 2D analogue, that is the model describes the square-to-rectangle phase transformations. In particular, our considerations are based on a modification of the following coupled system of PDEs for the evolution of displacements (u_1, u_2) and temperature T [8, 9]:

$$\frac{\partial^2 u_1}{\partial t^2} = \frac{\partial \sigma_{11}}{\partial x} + \frac{\sigma_{12}}{\partial y} + f_1, \quad \frac{\partial^2 u_2}{\partial t^2} = \frac{\partial \sigma_{12}}{\partial x} + \frac{\sigma_{22}}{\partial y} + f_2, \quad (6)$$

$$c_v \frac{\partial T}{\partial t} = k \left(\frac{\partial^2 T}{\partial x^2} + \frac{\partial^2 T}{\partial y^2} \right) + a_2 T e_2 \frac{\partial e_2}{\partial t} + g \quad (7)$$

with

$$\sigma_{11} = \frac{\sqrt{2}}{2} \rho (a_1 e_1 + a_2 (T - T_0) e_2 - a_4 e_2^3 + a_6 e_2^5) + \frac{d_2}{2} \nabla_x^2 e_2, \quad (8)$$

$$\sigma_{12} = \frac{1}{2} \rho a_3 e_3 = \sigma_{21}, \quad (9)$$

$$\sigma_{22} = \frac{\sqrt{2}}{2} \rho (a_1 e_1 - a_2 (T - T_0) e_2 + a_4 e_2^3 - a_6 e_2^5) + \frac{d_2}{2} \nabla_y^2 e_2 \quad (10)$$

for the case of nanowire specific geometry. We discuss the contributions of the surface stress and in this context analyze the differences in modelling bulk and nanowires. One of the applications of the nanowires discussed in this contribution stems from their integration in biomolecular technologies and we highlight the importance of the contributions of entropic elasticity [6] in such cases. Finally, we provide details on the extension of the models discussed here to include nonlocal effects allowing to account for size-dependent properties of the nanostructures [7]. In the above model, T_0 is the reference temperature, c_v and d_2 are material specific coefficients and other parameters have been defined in the previous section.

In this initial study, we focus on the mechanical field contributions. A more systematic coupling between the mechanical and thermal fields can easily be implemented as a direct extension of the proposed methodology. In this simplified case, by substituting

the free energy function into the conservation law of linear momentum, the governing equations for the dynamics of the system under consideration can be reduced to the following system:

$$\begin{aligned}\frac{\partial^2 u_1}{\partial t^2} &= \frac{\sqrt{2}}{2} \frac{\partial}{\partial x} (a_1 e_1 + a_2 (\theta - \theta_0) e_2 - a_4 e_2^3 + a_6 e_2^5) + \frac{1}{2} \frac{\partial}{\partial y} (a_3 e_3) + \sigma_x^g + f_1, \\ \frac{\partial^2 u_2}{\partial t^2} &= \frac{1}{2} \frac{\partial}{\partial x} (a_3 e_3) + \frac{\sqrt{2}}{2} \frac{\partial}{\partial x} (a_1 e_1 - a_2 (\theta - \theta_0) e_2 + a_4 e_2^3 - a_6 e_2^5) + \sigma_y^g + f_2,\end{aligned}\tag{11}$$

where

$$\sigma_x^g = k \left(\frac{\partial^4 u_1}{\partial x^4} - \frac{\partial^4 u_2}{\partial x^3 \partial y} + \frac{\partial^4 u_1}{\partial x^2 \partial y^2} - \frac{\partial^4 u_2}{\partial x \partial y^3} \right) \tag{12}$$

$$\sigma_y^g = k \left(-\frac{\partial^4 u_1}{\partial x^3 \partial y} + \frac{\partial^4 u_2}{\partial x^2 \partial y^2} + \frac{\partial^4 u_1}{\partial x \partial y^3} - \frac{\partial^4 u_2}{\partial y^4} \right) \tag{13}$$

Note that although the original model has been substantially simplified, it is still able to capture some basic features of the system dynamics.

4 Computational Implementation

Since the system has been simplified, it can be solved by the method of lines. The spatial discretization was carried out with the Chebyshev pseudo-spectral methodology supplemented by the Chebyshev-Lobatto quadrature rule. In particular, in the longitudinal direction with the boundaries of the computational domain denoted by z_a and z_b we choose a set of Chebyshev points $\{z_i\}$ as follows:

$$z_i = (z_b - z_a) \left(1 + \cos \left(\frac{\pi i}{N} \right) \right) / 2 + z_a, \quad i = 0, 1, \dots, N, \tag{14}$$

where $N + 1$ is the number of nodes chosen for the approximation. Based on these nodes, our approximations can be represented by the the following linear approximations:

$$\mu(z) = \sum_{i=0}^N \mu_i \phi_i(z), \tag{15}$$

where $\mu(z)$ is the corresponding component of the displacement function and μ_i is the function value at z_i , while $\phi_i(z)$ is the i^{th} interpolating polynomial associated with z_i which has the following property:

$$\phi_i(z_j) = \begin{cases} 1, & i = j, \\ 0, & i \neq j. \end{cases} \tag{16}$$

We note that if we have $\mu(z)$ approximately, the derivative $\partial\mu(z)/\partial z$ can be easily obtained by taking the derivative of the basis functions $\phi_i(z)$ with respect to z :

$$\frac{\partial\mu}{\partial z} = \sum_{i=0}^N \mu_i \frac{\partial\phi_i(z)}{\partial z}. \quad (17)$$

This allows us to reduce the problem to a matrix form

$$\mathbf{M}_z = \mathbf{D}\mathbf{M}, \quad (18)$$

with matrix \mathbf{D} determined by its elements as follows:

$$\mathbf{D}_{ij} = \begin{cases} \frac{2N^2 + 1}{6} & i = j = 0, \\ -\frac{2N^2 + 1}{6} & i = j = N, \\ -\frac{z_j}{2(1 - z_j^2)} & i = j = 1, 2, \dots, N - 1, \\ \frac{c_i}{c_j} \frac{(-1)^{i+j}}{(z_i - z_j)} & i \neq j, \quad i, j = 1, 2, \dots, N - 1, \end{cases} \quad (19)$$

where

$$c_i = \begin{cases} 2, & i = 0, N, \\ 1, & \text{otherwise.} \end{cases} \quad (20)$$

As already mentioned, we use the Chebyshev-Lobatto formulae for our quadrature rules in computing numerically the associated integrals. This was followed by the domain decomposition method as explained in Section 5. The resulting system, along with corresponding boundary conditions, has been reduced to a system of differential-algebraic equations which is solved with the second order backward differentiation formula:

$$\mathbf{M} \left(\frac{3}{2} \mathbf{X}^n - 2 \mathbf{X}^{n-1} + \frac{1}{2} \mathbf{X}^{n-2} \right) + \Delta t \mathbf{N}(\mathbf{t}_n, \mathbf{X}^n, \mathbf{V}(\mathbf{t}_n)) = \mathbf{0}, \quad (21)$$

where n denotes the current computational time layer. For each computational time layer, iterations have been carried out by using Newton's method.

We also confirmed our results with a finite element implementation.

5 Numerical Results

In what follows we report several preliminary results on modelling a Cu nanowire. In our experiments, we fix the length of the nanowire at $1 \mu m$ and looked at the initial stage of microstructure formation by using a coarse-grained model developed in Section 3, varying the diameter of the nanowire.

The computational parameters we used for all the computations reported in this contribution are given by:

$$a_2 = 4.80 \times 10^7 \text{ kg/s}^2 \text{ mK}, \quad a_4 = 6 \times 10^{11} \text{ kg/s}^2 \text{ m}, \quad a_6 = 4.5 \times 10^{13} \text{ kg/s}^2 \text{ m},$$

$$k = k_1 a_1, \quad a_1 = 3.0 \times 10^7 \text{ kg/s}^2 \text{ m}, \quad a_3 = 6.0 \times 10^7 \text{ kg/s}^2 \text{ m}.$$

The applied forces were set as $f_x = 7 \times 10^4$, $f_2 = 0$ and the boundary conditions were fixed (in particular, $u_1 = u_2 = 0$ were set on all boundaries).

In Fig. 1 we present the results obtained with the methodology described in the previous section where the entire nanowire was divided into two areas, corresponding to the “martensite plus” with $e_2 \approx 0.12$ and the “martensite minus” with $e_2 \approx -0.12$. The width of the nanowire in this case was 150 nm.

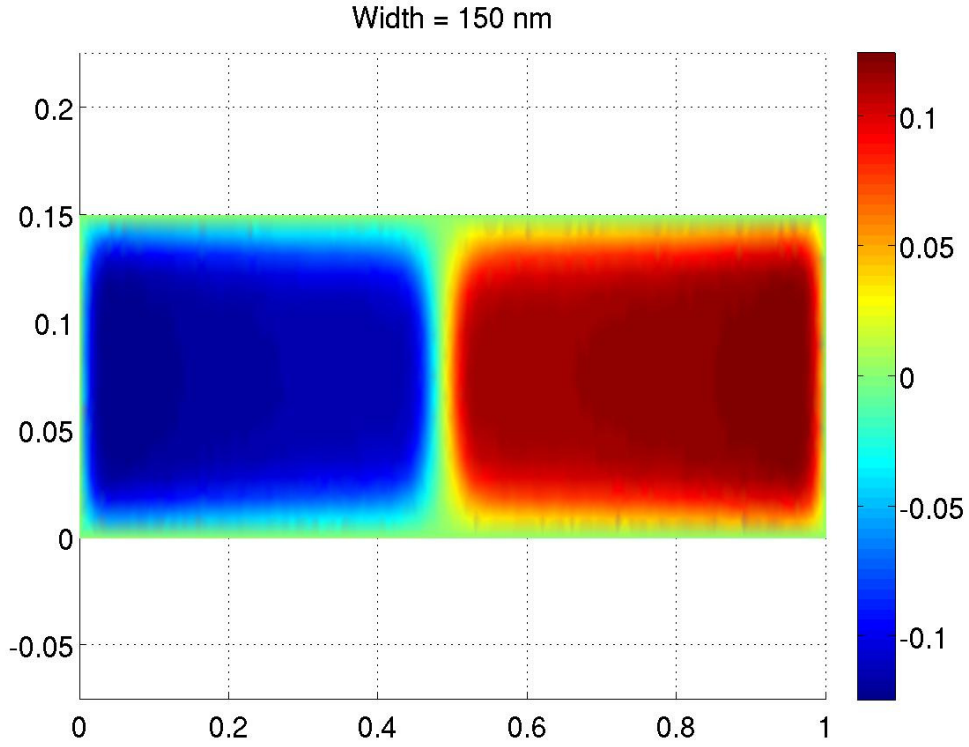


Figure 1: Initial stage of microstructure formation in the nanowire of 150 nm width and $k_1 = 10$.

In Fig. 2 and 3 we present the initial pattern formation for nanowires of smaller width, in particular with width of 100 nm and 80 nm, respectively. We observe that for all these cases the initial pattern formation is propagating towards the longitudinal boundaries of the structure, decaying with decrease in the nanowire width.

As Fig. 4 demonstrates that the above observation remains true even after decreasing the width of the nanowire to 50 nm.

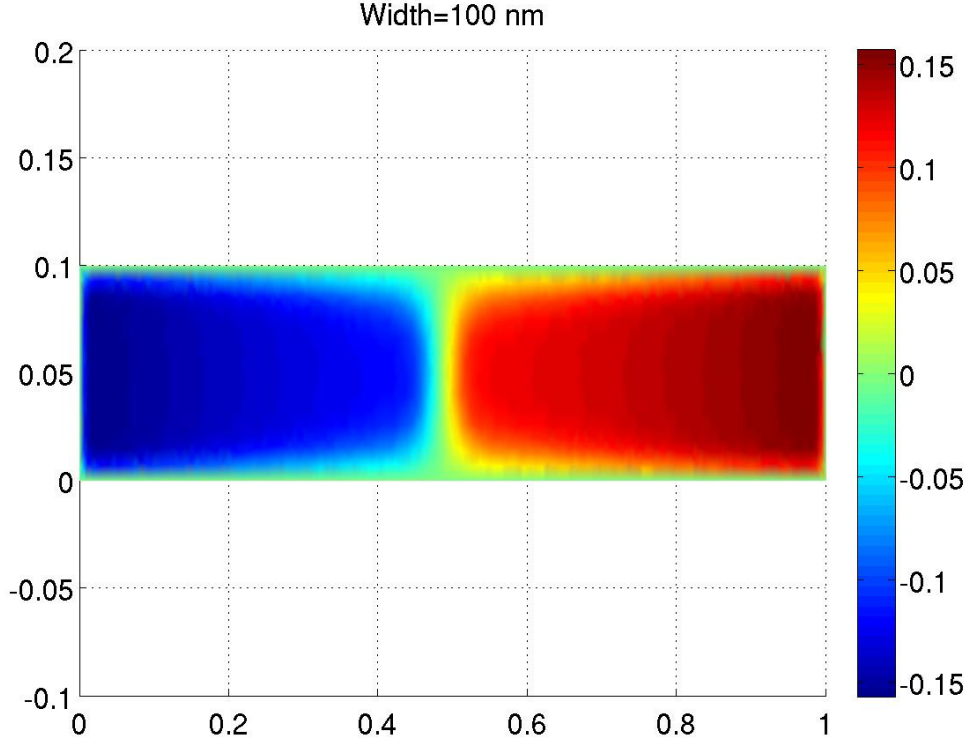


Figure 2: Initial stage of microstructure formation in the nanowire of 100 nm width and $k_1 = 10$.

The explanation of this phenomenon lies with the effect of surface energy.

In order to demonstrate it, we increased the value of coefficient k_1 from 10 to 1000 and carried out computations again for a nanowire of width 100nm. We observe that in this case, surface energy suppresses the pattern formation.

6 Conclusion

In this paper, we proposed a simplified two-dimensional model for studying finite length nanowires that may exhibit square to rectangle phase transformations. The model has been implemented by using the Chebyshev pseudo-spectral methodology combined with the domain decomposition method and second order backward differentiation. Based on this implementation we analyzed Cu nanowires with different diameter-length ratio. Our preliminary results indicated that for the range of diameter-length ratio studied here the initial pattern formation propagates towards the longitudinal boundaries of the structure when the nanowire width decreases. We provided an explanation of this phenomenon confirming that in all cases considered here surface energy suppresses the pattern formation.

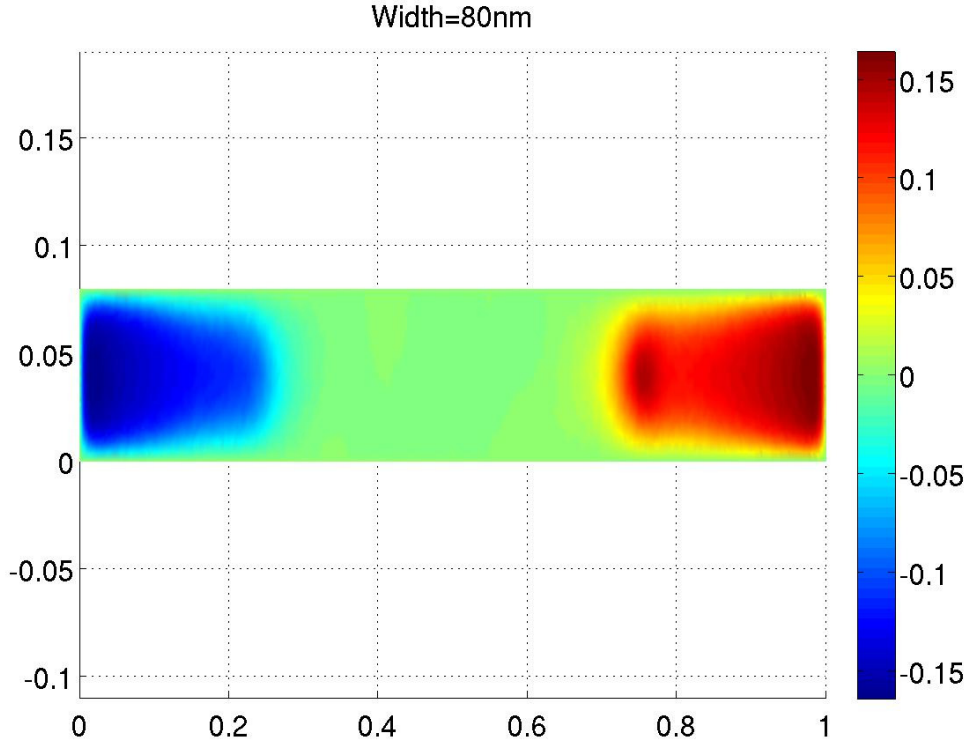


Figure 3: Initial stage of microstructure formation in the nanowire of 80 nm width and $k_1 = 10$.

References

- [1] K. Gall et al, “Tetragonal phase transformation in gold nanowires”, ASME J. of Engineering Materials and Technology, 127, 417–422, 2005.
- [2] W. Liang and M. Zhou, “Shape Memory Effect in Cu Nanowires”, Nano Lett., 5 (10), 2039 -2043, 2005.
- [3] D.R. Mahapatra and R.V.N. Melnik, “Three-dimensional mathematical models of phase transformation kinetics in shape memory alloys”, Dynamics of Continuous Discrete and Impulsive Systems. Series B - Applications & Algorithms, Vol. 2, Sp. Iss. SI, 557-562, 2005.
- [4] D.R. Mahapatra and R.V.N. Melnik, “Finite element approach to modelling evolution of 3D shape memory materials”, Mathematics and Computers in Simulation, 76(1-3), 141-148, 2007.
- [5] R.V.N. Melnik, A.J. Roberts, and K.A. Thomas, “Computing dynamics of copper-based SMA via centre manifold reduction of 3D models”, Computational Materials Science, 18 (3-4), 255268, 2000.
- [6] R.V.N. Melnik, D. Strunin, A.J. Roberts, “Nonlinear Analysis of Rubber-Based Polymeric Materials with Thermal Relaxation”, Numerical Heat Transfer A, 47(6), 549–569, 2005.

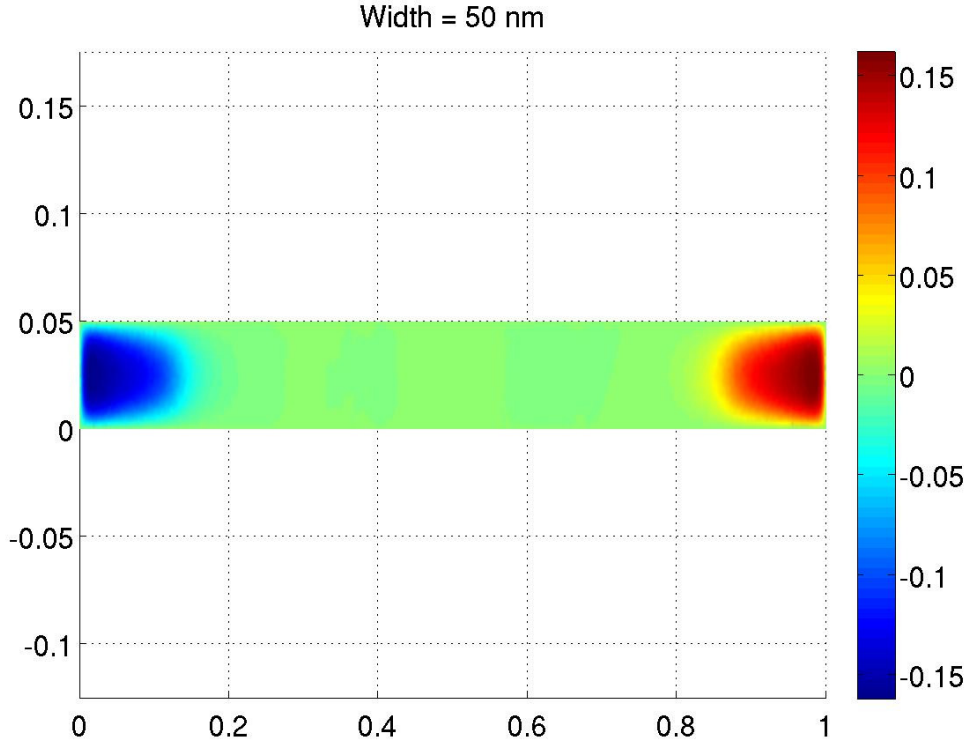


Figure 4: Initial stage of microstructure formation in the nanowire of 50 nm width and $k_1 = 10$.

- [7] J. Peddieson, G.R. Buchanan, R.P. McNitt, “Application of nonlocal continuum models to nanotechnology”, *Int. J. Eng. Sci.*, 41, 305–312, 2003.
- [8] L. X. Wang and R.V.N. Melnik, “Model reduction applied to square to rectangular martensitic transformations using proper orthogonal decomposition”, *Applied Numerical Mathematics*, 57(5-7), 510-520, 2007.
- [9] L. X. Wang and R.V.N. Melnik, “Finite volume analysis of nonlinear thermo-mechanical dynamics of shape memory alloys”, *Heat and Mass Transfer*, 43(6), 535–546, 2007.
- [10] Zhang, L. and H. Huang, Structural transformation of ZnO nanowires, *Appl. Phys. Lett.*, 90, 023115, 2007.

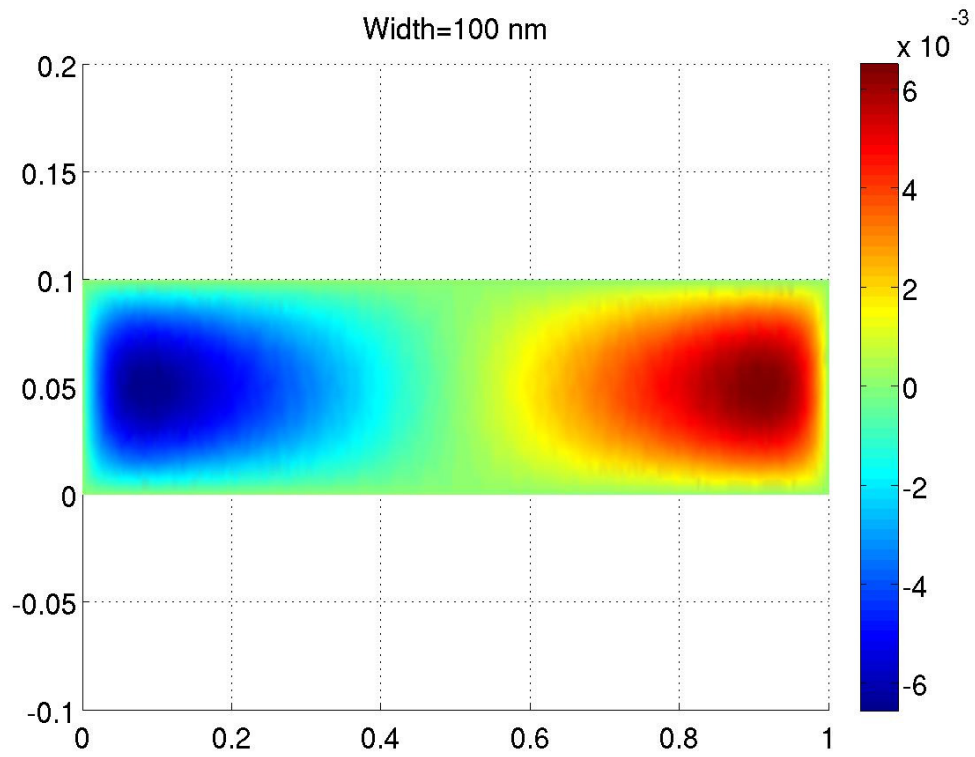


Figure 5: Initial stage of microstructure formation in the nanowire of 100 nm width and $k_1 = 1000$.

Proceedings of the Sixth International Conference on Engineering Computational Technology

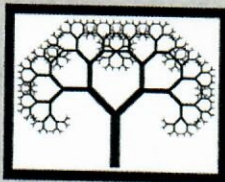
Edited by M. Papadrakakis and B.H.V. Topping

This book contains the summaries of the contributed papers presented at the Sixth International Conference on Engineering Computational Technology, held in Athens, Greece, 2-5 September 2008.

The full length papers are available in electronic format on the accompanying CD-ROM. The topics covered include:

- High Performance Computing
- Fluid-Structure Interaction
- Quantification of Uncertainty
- Interfaces
- Decision Making
- Multiscale Simulation
- Mesh Generation and Adaption
- Information Modeling
- Computational Linear Algebra
- Genetic Algorithms
- Parallel Computations
- Distributed Computing
- Computational Fluid Dynamics
- Optimization
- Meshless Methods
- Discrete Finite Element Methods
- Finite Element Solver Technology
- Boundary Element Methods
- Nano-Mechanics
- Particle Thermodynamics
- Computer Aided Engineering
- Computer Vision
- Biomedical Engineering
- Biomechanics
- Rock Mechanics
- Soil-Structure Interaction
- Geotechnical Engineering
- Environmental Engineering

A keyword and author index is provided both in this book and on the CD-ROM.



Civil-Comp Press

ISBN	978-1-905088-24-9	Book
ISBN	978-1-905088-25-6	CD-ROM
ISBN	978-1-905088-26-3	Combined Set

*Proceedings of
The Sixth International Conference on
Engineering Computational Technology*

CIVIL-COMP CONFER
25
1983-2008



Civil-Comp Press

ISBN 978-1-905088-24-9 Book
ISBN 978-1-905088-25-6 CD-ROM
ISBN 978-1-905088-26-3 Set

COMPACT
disc
DATA STORAGE

© Copyright 2008
Civil-Comp Ltd.
All Rights Reserved

*Edited by M. Papadrakakis and B.H.V. Topping
Athens - Greece
2-5 September 2008*